Int. J. New. Chem., 2023, Vol. 10, Issue 2, pp. 65-83.

International Journal of New Chemistry

Published online 2020 in http://www.ijnc.ir/.

Open Access

Print ISSN: 2645-7237

Online ISSN: 2383-188x

Original Research Article

Synthesis and characterization of poly methyl methacrylate-b-polystyrene copolymer/ multi -walled carbon nanotubes via ATRP and NMRP techniques

Mojtaba Abbasian[1], Saber Ghasemi Karaj-Abad [2,*], Mehdi Hosseinzadeh [2,*], Shiva Asadi[2]
and Solmaz Esmaeily Shoja[2]

[1] Department of Chemical Engineering, University of Bonab, Bonab, Iran

E-mail address: m_abbasian@pnu.ac.ir, m_abbasian20@yahoo.com

[2] Department of Chemistry, Payame Noor University, P. O. Box: 19395-3697 Tehran, Iran

[3]Mehdi Hosseinzadeh, Marand Faculty of Technical and Engineering, University of Tabriz, Tabriz, Iran

[4] Lab. of Materials, Faculty of Engineering, Islamic Azad University, Bonab branch, Bonab, Iran.

Received: 2021-11-01 *Accepted: 2022-02-15* *Published: 2023-03-02*

ABSTRACT

Graft polymerization of polymethyl methacrylate–block-polystyrene (PMMA-b-PSt) has been carried out from the surface of multi-walled carbon nanotubes (MWCNTs) using living radical polymerization methods. For this purpose, the first surfaces of MWCNTs were functionalized by acid treatment and then acylated by thionyl chloride (SOCl2). After that, the toluene unit was successfully grafted onto MWCNTs side walls by Friedel craft acylation reaction in the presence of ZnO as a catalyst. The obtained nanotube-toluene was brominated by N-bromosuccinimide (NBS). This brominated nanotube-toluene was used as a macroinitiator for atom transfer radical polymerization (ATRP) of methyl methacrylate (MMA) in the presence of the CuBr/ 2, 2′-bipyridine (bpy) catalyst system to obtain MWCNTs-graft-polymethyl methacrylate (MWCNTs-g-PMMA). Then 1-hydroxy-2, 2, 6, 6-tetramethyl-piperidine (TEMPO-OH) obtained by reduction of 2, 2, 6, 6-tetramethyl-piperidinyl-1-oxy (TEMPO) with sodium ascorbate. The bromine groups at the end of PMMA have converted to nitroxide mediated groups by coupling with TEMPO-OH to yield MWCNTs terminated with a TEMPO unit (MWCNTs-PMMA-TEMPO). At last, the resulting macroinitiator was employed for ‘living’ free-radical polymerization of styrene (St) by nitroxide-mediated radical polymerization (NMRP) to form MWCNTs-g-(PMMA-b-PS). Fourier transform infrared (FT-IR) spectroscopy, transmission electron microscopy (TEM), scanning electron microscopy (SEM), differential scanning calorimetry (DSC), and thermogravimetric analysis (TGA) show the effective grafting of MMA and styrene onto the MWCNTs.

Keywords: Multi-walled carbon nanotube functionalization, ATRP, Polystyrene, NMRP

***Corresponding Author:** sg.chemist1988@gmail.com,
ghasemi_s@yahoo.com, mh_1268@yahoo.com:**

1. Introduction

Expansive research has been conducted for the surface treatment of carbon nanotubes chiefly to increase their chemical amenability and dissolution features [1-5]. Recently, the preparation of grafted polymers with end-functionalized on a substrate like SWCNT and MWCNT has attracted the attention of many researchers due to their new structure and features [6, 7]. Grafted polymers with end-functionalized are communally prepared by the covalent connection of polymer chains to a substrate (e.g., MWCNTs) by either "grafting from" or "grafting to" approaches. The "grafting to" paths involve the grafting between end-functionalized polymer chains and an appropriate substrate. The "grafting from" path necessities immobility of initiators onto the substrate chased by the in-situ surface-initiated polymerizations of the polymeric chains [8]. Exclusively, in the "grafting from" technique, the molecular weight distribution and molecular weight of the grafted polymers could be controlled via radical polymerization. In the past few decades, many investigators have afforded to use controlled/living polymerization approaches to synthesize nanocomposite polymers with well-defined structures. Controlled/living radical polymerization (CLRP) provides the preparation of polymers with narrow molecular weight distributions (MWDs), predestinated molecular weights and variant complex architectures. Recently, significant progress has been made in controlled radical polymerization to prepare tailor-build polymers with predicted molecular weights and well-defined architecture [9]. Several approaches have been developed to obtain this control: nitroxide-mediated radical polymerization (NMRP) [10-12], atom transfer radical polymerization (ATRP) [13-17], and reversible addition- fragmentation process (RAFT) [18-20]. Nitroxide-mediated radical polymerization technique is a controlled free radical methodology which presents the preparation of graft and star copolymers with a controlled molecular weight under moderate conditions. This polymerization technique is originated from the conventional radical initiator (e.g., B.P.O) in the adjacency of stable nitroxide radical (e.g., TEMPO). In this type of proceeding, the diffusing species (Pn°) reacts with a stable radical (X°). The produced dormant species (Pn-X) can become then reversibly separate to revive the free radicals. Once Pn° forms, it can react with a monomer, M, and propagate further. The most important utilized stable radicals have been nitroxides, chiefly 2, 2, 6, 6-tetramethylpiperidinoxy (TEMPO) [21-23]. A superiority of ‘living’ free-radical polymerization (LFRP) is the synthesis of graft copolymers compared with other copolymerization methods such as anionic polymerization. And also, the terminative groups in the ‘living’ free-radical polymerization are in stable condition at room temperature, and previous polymer materials could be isolated, kept, and utilized as required. In addition, in anionic polymerization, accurate conditions for polymerizations are needed [24]. ATRP is catalyzed by transition metal (such as copper, nickel, ruthenium, etc.) halide complexes with 2,2´-bipyridine (bpy) derivatives for polymerization of variant monomers, such as methacrylates, styrene, acrylates, etc., has been presented in our laboratory and other laboratories [13,15].ATRP provides equivalency between active propagating radicals and dormant alkyl halides to preserve a low concentration of active species. The activated radical species can either diffuse or be deactivated to revive the dormant species. ATRP also has excellence in providing an extensive range of initiators. Alkyl halides with radical stabilizing substituents such as carbonyl, cyano, or aryl group adjacent to the C-X can be utilized as the initiator. Any compound, including macromolecular species, can potentially initiate ATRP as long as they contain activated halogen atoms [25].Indeed, in situ surface-initiated controlled polymerization of SWCNT and MWCNT has been recently introduced utilizing either ATRP [26, 27] or NMRP [28]. Growth of polymer chains from covalently attached surface initiators using the "grafting-from" method and incorporating two approaches, ATRP and NMRP are the best proceeding to achieving polymer brushes on any surface. Until now, gold, silicon, and clay surfaces have been utilized to develop polymers through surface-initiated polymerization (SIP). In this present study, we explain the surface-initiated atom transfer radical polymerization (SI-ATRP) of MMA and NMRP of St from MWCNTs. For this purpose, the first surfaces of MWCNTs were functionalized by acid treatment and then acylated by thionyl chloride ($SOCl_2$). After that Grafting of the toluene unit onto MWCNTs side walls was successfully done by *Friedel Craft acylation* reaction. We used the obtained nanotube-toluene and NBS to obtain nanotube-toluene with bromine groups. This brominated nanotube-toluene was used as an ATRP macroinitiator for the polymerization of MMT in the presence of the CuBr/bpy catalyst system. The bromine groups at the end of PMMA were shifted to nitroxide mediated groups by coupling with (TEMPO-OH). The resulting macroinitiator (MWCNT-PMMA-TEMPO) for 'living' free-radical polymerization was then heated in the adjacency of St to form MWCNTs-g-(PMMA-b-PSt).

2. Experimental

2.1. Materials

TEMPO was synthesized by the method introduced by our research group previously [29, 30]. Sodium-L (+)-ascorbate was achieved from Merck (Darmstadt, Germany) and utilized without further refinement. The MWCNTs was prepared by the Research Institute of Petroleum Industry (Tehran, Iran and diameter ≈ 8 nm, length ≈ 50 μm). Styrene monomer was obtained from the Petrochemical Company of Tabriz (Tabriz, Iran). Methylmethacrylate (Aldrich) monomers were purified through drying by CaH_2 for 3 days and then distillation. Azobisisobutyronitrile (AIBN) initiator (Toronto Research Company), was dried at room temperature by refluxing over sodium and finally kept in a freezer. Toluene, chloroform, carbon tetrachloride, tetrahydrofuran (THF), and Triethylamine were acquired from Merck. They were dried over CaH_2 and distilled before use. CuCl (I) (Merck) purified in 100ml glacial acetic acid. Bipyridine (Merck), N, N-(dimethylamino), pyridine (DMAP), and NBS, ZnO, thionyl chloride ($SOCl_2$) were obtained from Aldrich Chemical Company used as received.

2.2. Characterization

An ultrasonic cleaning bath (HD-3200, Ultrasonic Homogenizer, BANDELIN, Germany), operating at 50 kHz, was used. FT-IR spectrum of the specimens were examined on a Shimadzu 8101M FT-IR spectrometer (Shimadzu, Japan, Kyoto). The specimens were synthesized by grinding the dry powders with KBr and compressing the mixture into disks. The disks were kept in desiccators to eliminate moisture absorption. The spectrum was employed at room temperature, in the range of 400-4000 cm^{-1}. The thermogravimetric analysis (TGA) was accomplished on a TGA instrument Q600 (TA

Instruments, USA) at a heating of 10°C /min in flow N_2. DSC analyses was accomplished using a NETZSCH DSC 200 F3 Maia (NETZSCH, Germany). The specimen was first heated to 130°C and stored for about 5 min to avoid thermal history. Afterward, this process was then repeated to 250 °C at a rate of 10 °C/min. Scanning electron microscopy (SEM) images were achieved on SEM MAG 50.00 KX system. Transmission electron microscopy (TEM) was accomplished on Philips CM10 TEM (Philips Electron Optics, The Netherlands, Eindhoven) microscope and recorded at 100 kV.

2.3. Acid treatment of MWCNTs

A 100-mL glass flask fitted with a flux condenser and a magnetic stirrer was charged with purified MWCNTs in the previous step (0.90 g), and a mixture (3:1 v/v) of H_2SO_4 (20 mL, 96–98%) and HNO_3 (40 mL, 67%). The content of the flask was then sonicated and refluxed through an ultrasonic bath at 100 °C for about 5 hr to open aggregation of nanotubes and represent functional carboxylic acid groups on the surface of MWCNTs. After the end of this time, several times dilution was then exerted to the reaction mixture, in order to terminate oxidation reaction. The obtained product was washed several times with distilled water until the pH water became 7. Accordingly, the product was dried in a vacuum oven at 60 °C for about 12 hrs. The obtained product was 0.5 gr and attributed as carboxylated MWCNTs (MWCNTs–COOH) [31].

2.4. Acylation of carboxylated MWCNTs

The produced CNTs-COOH (0.5 g) in DCM (40 ml), then aniline (1.5 g), DCC (31.8 mmol, 6.61 g) and DMAP (3.18 mmol, 0.39 g) were added, respectively. The mixture was refluxed for 24 hrs at 100°C with intense mechanical stirring under N_2 protection. Following that, the material was washed with DCM and vacuum-dried at room temperature to give carbonyl chloride functionalized MWNT (MWCNTs-COCl) [31].

2.5. Synthesis of MWCNT-toluene

26 gr of toluene to the mixture of 10 g ZnO powder was added and 3gr of obtained MWCNT-COCl was stirred with a magnetic stirrer for about 24 hr at room temperature. Afterward, the Solid bulk was washed with THF to avoid any contains of unwanted toluene. Black solid mixture was washed with 30 mL of 0.1 M HNO_3 to eliminate ZnO. Accordingly, the toluene grafted MWCNTs with distilled water were washed and dried in the oven under vacuum at 60 °C for 5 h.

2.6. Synthesis of ATRP initiator on MWCNTs surfaces

A 100 mL flask comprising MWCNTs-toluene (0.30 g), anhydrous CCl_4 (10.0 mL), NBS (0.4 g), and AIBN (0.06 g) was emptied and three times filled with argon gasses. Subsequently, (2g) of MWCNTs-toluene dissolved in 30 mL of anhydrous CCl_4 was added dropwise. It was emptied and three times filled with argon gasses. The resulting mixture was stirred at 70°C temperature for 3 h. Then the solid product was disserted from the mixture by purification and washed several times with 100 mL of DCM. The dark solid was accumulated and dried overnight under a vacuum at 40°C to produce MWCNTs-Br.

2.7. ATRP reaction of MMA from MWCNTs surfaces

25.0 mg of MWCNTs-Br, 0.25 mL of toluene, 7.2 mg (0.050 mmol) of CuBr, and 8.7 mg (0.050 mmol) of bpy, were added to the solution and sonicated for 15 min. Then, 5 ml of MMA monomer into the flask utilizing a syringe was injected and plunged in an oil bath at 90°C for 24 hr. At the end of this time, the viscosity of the reaction gradually increased. Finally, the mixture was purified and washed with toluene and DCM several times to remove the monomer and dried in a vacuum at 60 °C for 12 h. (Scheme 1)

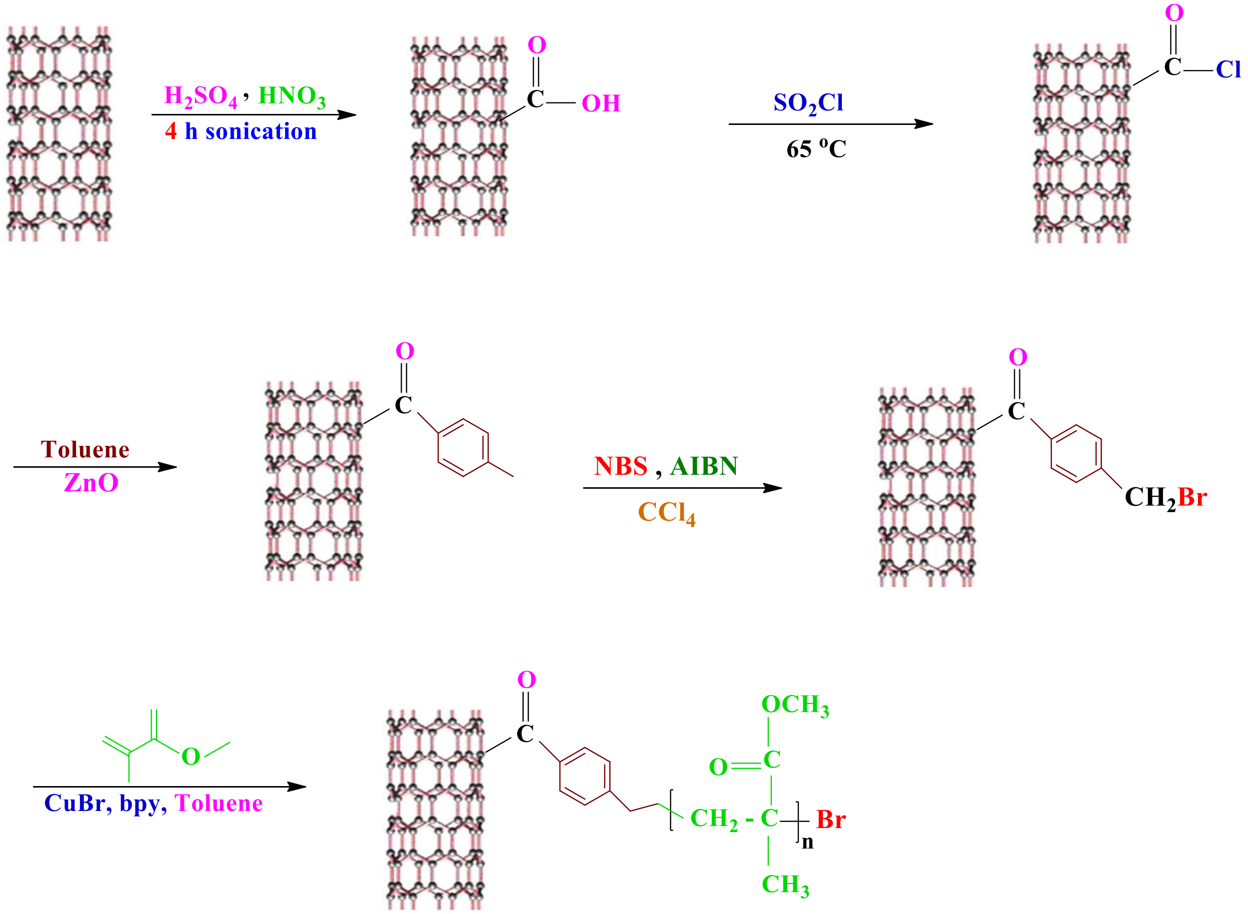

Scheme 1: ATRP reaction of MMA onto MWCNTs surfaces

2.8. Preparation of TEMP-OH by reduction of TEMPO

Reduction of TEMPO to TEMP-OH was prepared according to relevant reference [32, 33]

2.9. Synthesis of MWCNT- g-PMMA-TEMPO Macroinitiator

In a two-neck round-bottom flask equipped with condenser and a magnetic stirrer, TEMPO-OH (0.051 gr) in anhydrous N, N-dimethylformamide (DMF, 1mL was dissolved) and added under N_2 atmosphere to 8.0 mg hexane-washed NaH. The mixture was stirred for 30 min, and then 1g MWNT-MMA was added under N_2 and refluxed for

24 h. The reaction was finished by flowing the flask's content into a deal amount of acidic methanol. The solid was purified and dried in a vacuum.

2.9. NMP Polymerization of St onto MWCNT-g-PMMA-TEMPO

A two-neck round-bottom flask fitted with a condenser and a magnetic stirrer, 0.4 gr of macroinitiator (*MWCNT- g-PMMA-TEMPO*) and 5 mL (0.043 mmol) of St were placed in an ampoule degassed. The solution was stirred and heated at 125°C. The viscosity of the reaction during the reaction increased dramatically. After 14 h, the solution was dissolved in 10 mL CH_2Cl_2 and precipitated in 50 mL methanol for 24h. The crude product was dried in a vacuum. (Scheme 2)

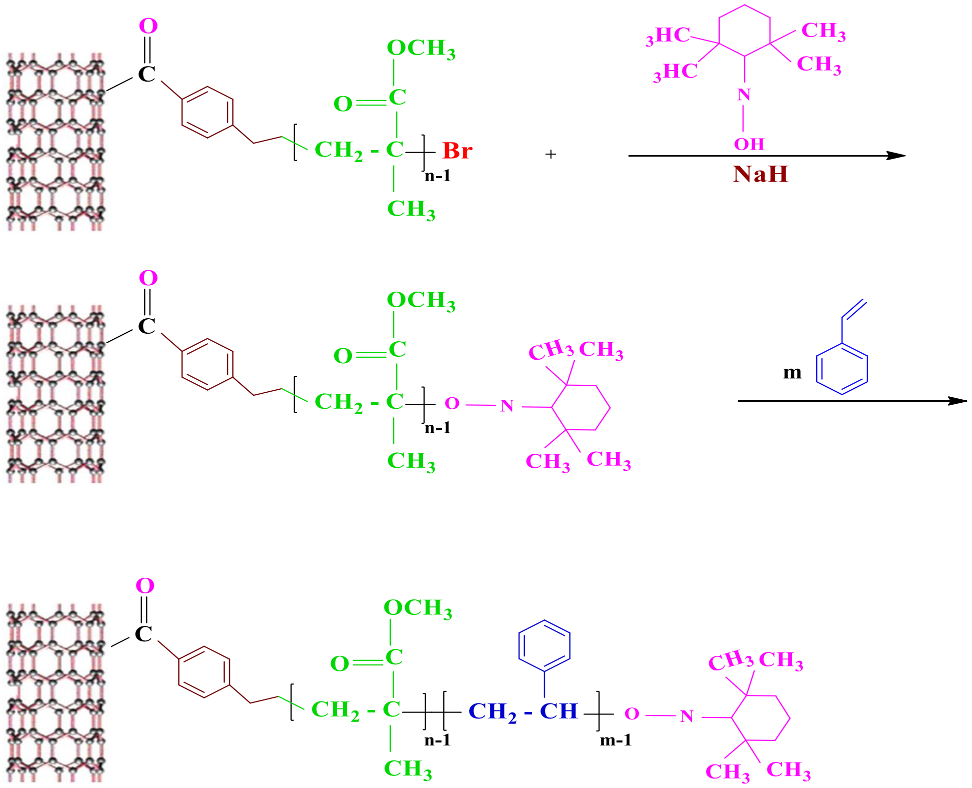

Scheme 2: NMRP reaction of *St* from MWCNTs-*g*-PMMA surfaces

3. Results and discussion

3.1. Preparation of ATRP macroinitiator

In this present project, surfaces of MWCNTs were grafted respectively by PMMA and PSt using ATRP and NMP. To carry out ATRP, the need for ATRP special initiator is required. So, an ATRP macroinitiator was synthesized in four steps: 1) acid treatment, 2) acylation of carboxylated MWCNTs, 3) toluene -grafted MWCNTs via *Friedel Craft acylation reaction,* and 4) bromination reaction by NBS. Figure 1 displays FT-IR spectra for materials obtained in four stages. As it is seen, the manifestation of a weak band at 771 cm^{-1} is attributed to the presence of a C-Cl bond related to MWCNT-CO-Cl [(Figure, 1(b)]. Also, in Figure 1(c), the peaks showed at 680 cm^{-1} and 1640 cm^{-1} assigned to the benzene ring of toluene, and the band at 1700 cm^{-1} assigned to ketone (C=O stretching) connection between the benzene ring of the toluene and MWCNTs. In Figure1 (d), observed peaks at 628 cm^{-1} and 1173 cm^{-1} are owing to bending and stretching vibration of $–CH_2Br$.

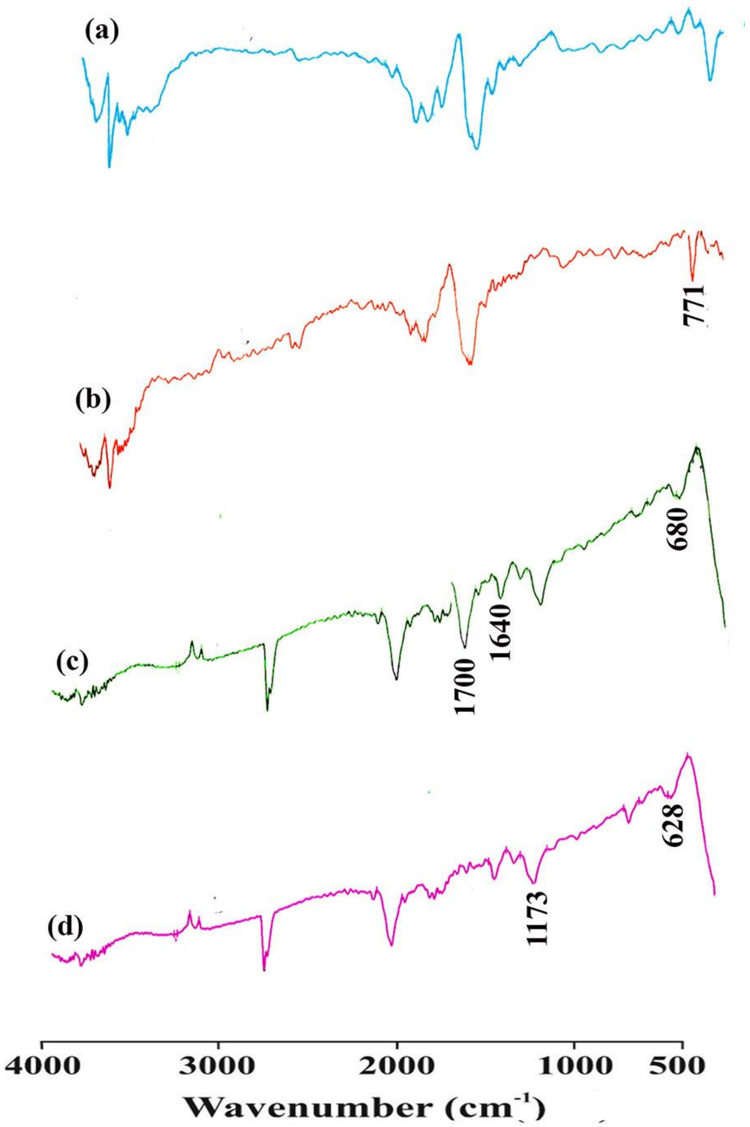

Figure 1: FT-IR spectra of primary MWCNTs (a), acylated MWCNTs (b), toluene grafted MWCNTs (c) and ATRP initiator created on MWCNTs surfaces (d)

3.2. Graft of MMT onto MWCNTs by ATRP (MWCNT-g-PMMA)

Figure 2 shows spectra for MWCNT-g-PMMA (a), MWCNT-g-PMMA-TEMPO (b), and MWCNT-g-PMMA-b-PS. In Figure 2(a), the peaks at 1772 cm^{-1}, 1650 cm^{-1} ,and 1220 cm^{-1} are related to carbonyl, -C=C- and C-O of the MMA segments.

3.4. Synthesis of MWCNT- g-PMMA-TEMPO Macroinitiator

Firstly, to make the active sites on PMMA, TEMPO was added to MWCNT-*g*-PMMA to give the MWCNT-*g*-PMMA-TEMPO macroinitiator. The FTIR spectra of macroinitiator MWCNT-g-PMMA-TEMPO indicates an absorption peak at 1560 cm^{-1}, which is assigned to the methyl bond of TEMPO (Figure 2b).

3.5. NMRP of St onto MWCNT-g-PMMA-TEMPO

TEMPO is a radical absorbent that couples with a carbon-centered radical at propagation confined reaction rate. The reversibility of the reaction presents that TEMPO is an effective intermediary in controlled/ living radical polymerization. Although after attachment to MWCNT, the movability of TEMPO would be reduced, it should still be high enough to trap carbon-centered diffusing radicals to produce polymer grafted MWCNT. Radical polymerization of St was performed in bulk in the adjacency of MWCNTs-g-PMMA-TEMPO, started with thermal initiation of monomer at 125°C [28]. For examination, the blank investigations performed in the adjacency of TEMPO onto PSt are also included. FTIR spectra of MWCNT-g-PMMA-b-PS are given in Figure 2 (c). In the spectrum, the band at 1581 cm^{-1} was owing to C=C stretch in the walls of MWNT, and the peak at 1768 cm^{-1} was owing to the C=O stretching mode of the ester, which was similar to that of MWNT-TEMPO. The peaks at 2950 and 2885 were related to the C-H stretching mode in the alkyl chains, and the band at 1352 was related to the C-H bending mode. The manifestation of these novel peaks demonstrated that PSt was covalently coupling to the surfaces of the MWCNTs.

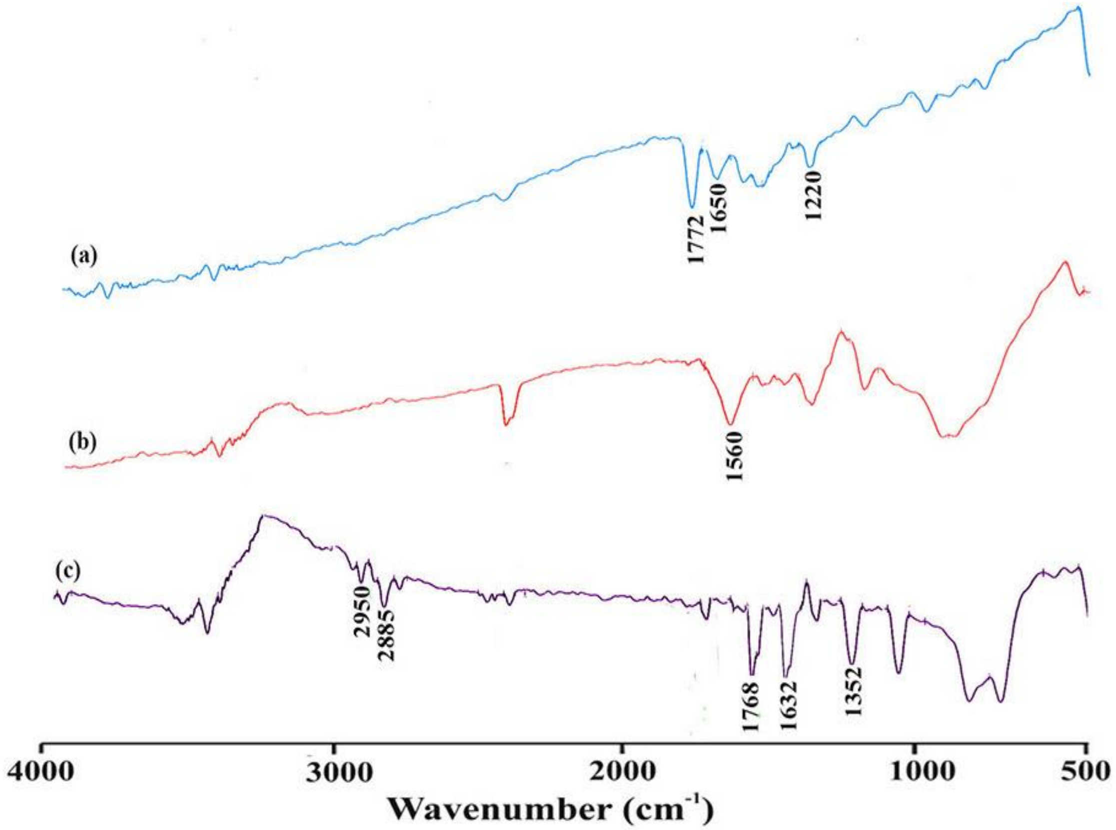

Figure 2: FT-IR spectra of MWCNTs-*g*-PMMA (a), MWCNTs-PMMA-*g*-TEMPO (b) and MWCNT-*g*-PMMA-b-PSt (c)

3.6. Thermal stability of PS grafted onto MWCNT-g-PMMA

The TGA analyses of MWCNT-g-PMMA in the adjacency of air demonstrated two specific decompositions in the temperature range at 110-230 °C and 410-550 °C attributing to surface grown polymer and MWCNTs, respectively. The surface grown PMMA decomposes at T_d = 160°C, while PMMA nano-fibers was 300°C and decomposed in a single step. Moreover, the residue values of MWCNT-g- PMMA are 35 % at 600°C. Since the MWCNT is stable at 600°C, PMMA is perfectly decomposed at 450°C, and the residue mass of PMMA-*g*-MWCNT is identical to the content of MWCNTs in MWCNTs -*g*- PMMA. TGA analysis indicated rapid weight loss of MWCNTs-g-PMMA-b-PSt at around 430°C as an initiator, indicating about 24% polymer weight loss under the identical condition. The results demonstrate that the thermal degradation of PSt in PS-g-MMA-MWNT is delayed by the incorporating of MWCNTs into PS as covalent connecting for the sake of the restriction effect of MWCNTs on the PSt chains and the high thermal stability of MWCNTs in *MWCNT-g-PMMA*-b-PSt. This procedure is permanent with the betterment in the thermal stability of poly (MMA) by nanotubes.

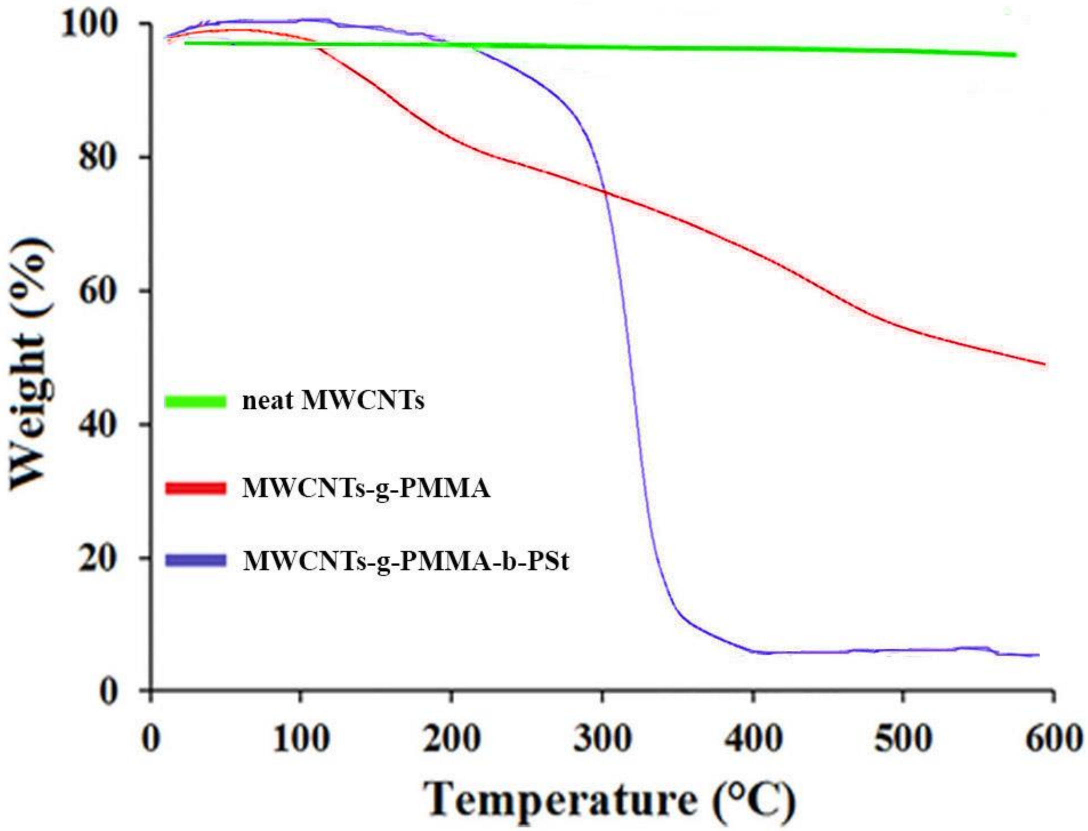

Figure 3: TGA curves of pristine MWCNT, MWCNT-g-PMMA and MWCNT-g-PMMA-b-PSt

3.7. Thermal behavior of grafted PS onto MWCNT-g-PMMA

In generally, the addition of CNTs can improve the glass-transition temperature (T_g) of a polymer matrix in a composite. Figure 4 indicates the DSC curves of MWCNT-g-PMMA and MWCNT-g-PMMA-PSt. It is obvious that the T_g of the PSt chains in MWCNT-g-PMMA-b-PSt shifts to a higher temperature (90°C) than that of neat PSt (50°C). The reason could be that the connection of MWCNTs into PSt via covalent bonding confines the segmental chain motions of PSt macromolecules. This phenomenon has also been observed in polymer-grafted metal nanoparticles. Furthermore, the PMMA electrospum nono-fibers demonstrated an endotherm in the first heating cycle, showing water absorbed that might be responsible for the lower T_g explored because of it could serve as a plasticizer. DSC analysis of *MWCNT-g-PMMA* nanocomposite presented a T_g at 120°C.

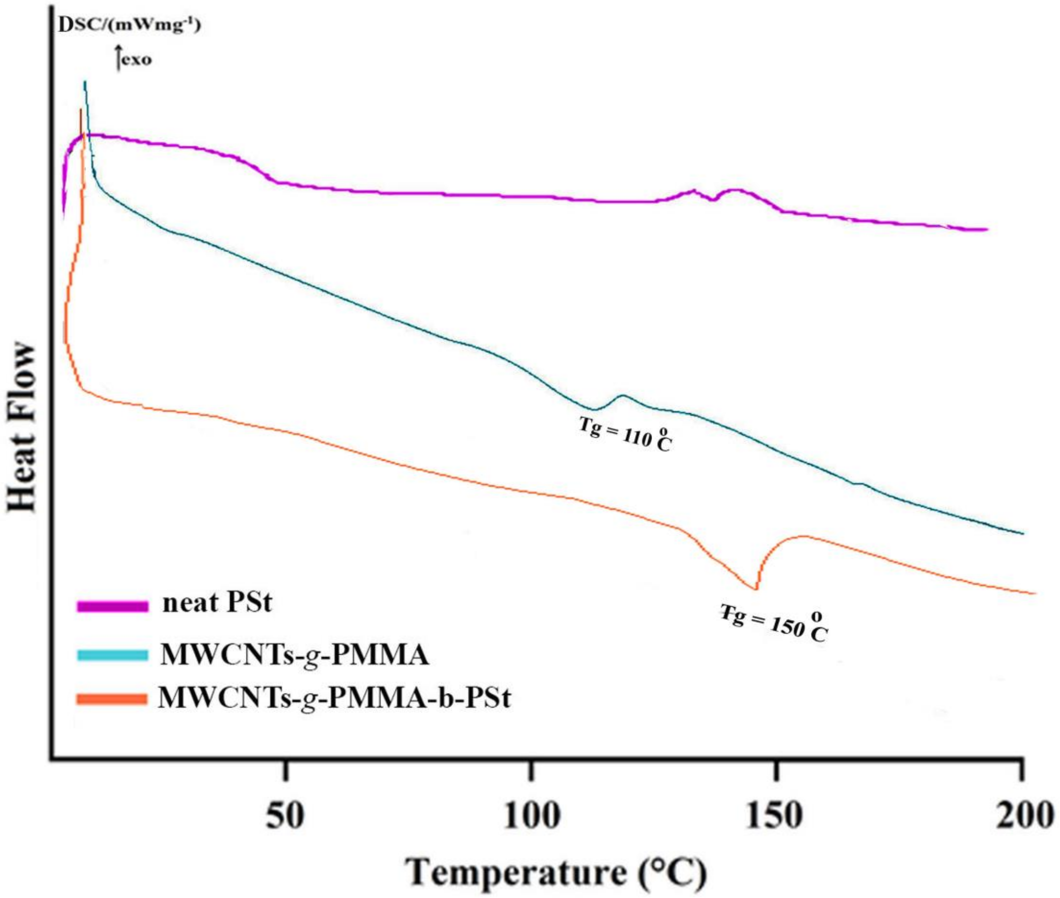

Figure 4: DSC traces of the neat PSt, MWCNT-g-PMMA and MWCNT-g-PMMA-b-PSt

3.8. SEM image of MWCNT-g-PMMA-b-PSt

SEM micrographs for MWCNT-g-PMMA and MWCNT-g-PMMA-b-PSt demonstrate the formation of nano-fibers with bead-free and fiber-bead-free morphologies. The characterizations, as mentioned above effectually indicate that the PSt and PMMA chains have been covalently attached to the nanotubes. Examinations of SEM microscopy could present further direct evidence. In the SEM image of crude MWCNTs, there are large quantities of neat nanotubes bundles, and the number of impurities containing graphite, amorphous carbon and catalyst particles.

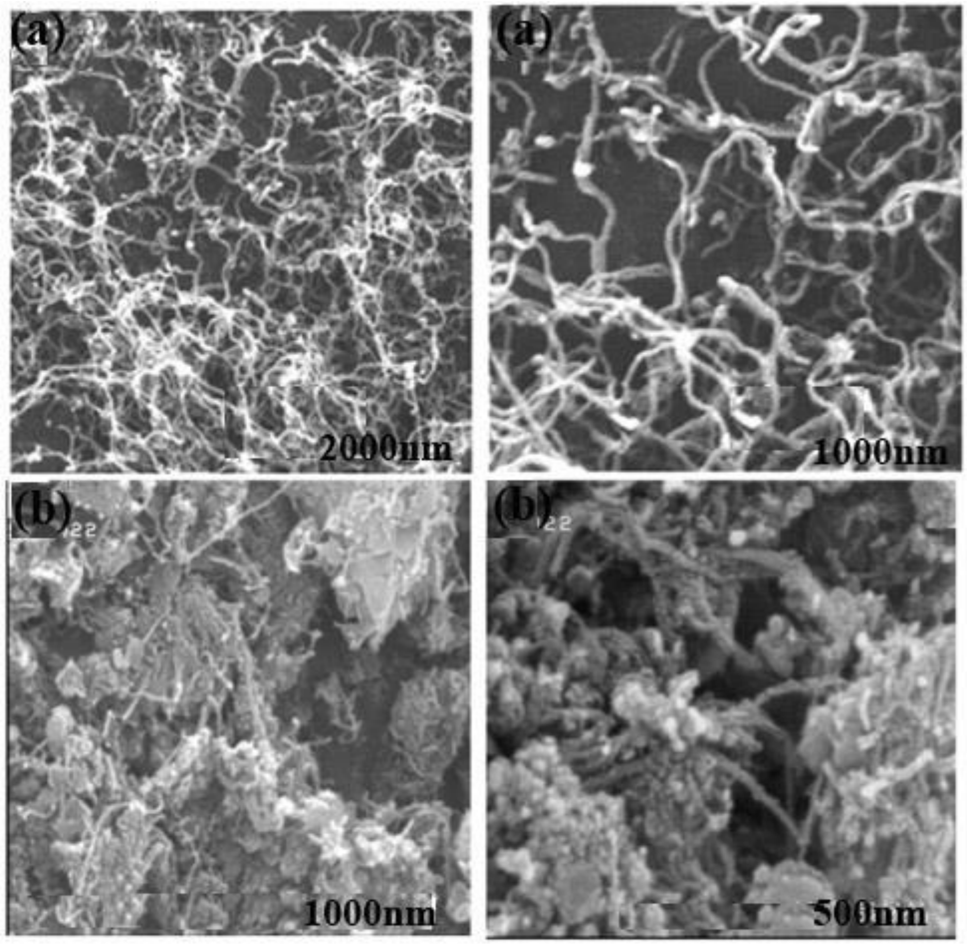

Figure 5: SEM image of MWCNT-*g*-PMMA (a) and MWCNT-*g*-PMMA-b-PSt (b)

3.9. TEM investigation of MWCNT-g-PMMA-b-PSt

MWCNT-*g*-PMMA-b-PSt demonstrates relatively rough surfaces along the nanotube axis. A uniform and thin layer of a shell cover the outer wall of every exclusive MWNT along its length, forming so-called core-shell structures. Emphasizing that the thickness of the PSt layer on the apex of the nanotube appears larger than that on the outer wall of the nanotube for the sake of the many more reaction sites there. The results confirm that the initiation and dissemination of polymerization were created not only at the apexes, but as well as on the outer walls of the CNTs. Furthermore, the coaxial nanostructure of the final PSt-g-MWNT is demonstrated, and it could be considered a novel kind of molecular nanocomposite due to the covalent bonding between the core and the shell.

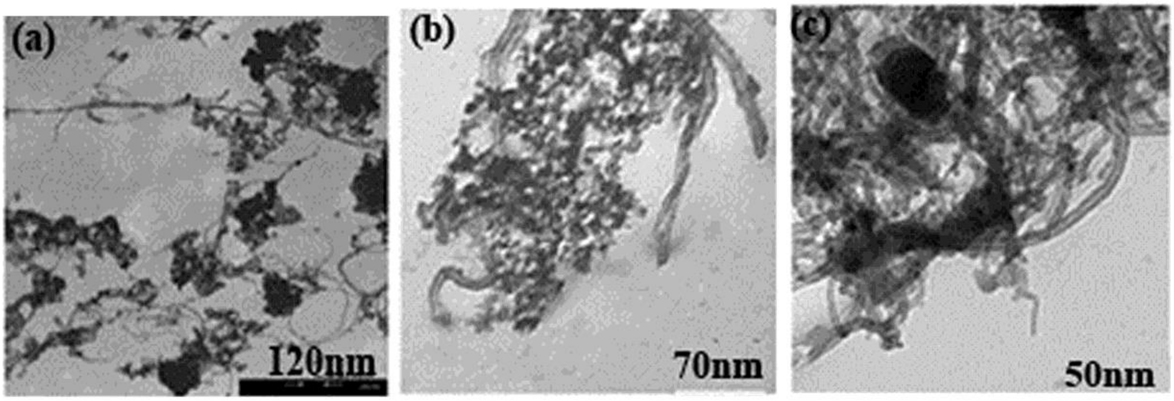

Figure 6: Transmission electron micrographs of (a) pristine MWCNTs, MWCNT-g-PMMA (b) and MWCNT-g-PMMA-b-PSt(c)

4. Conclusion

Surfaces of MWCNTs were successfully modified by graft polymerization of PMMA-b-PSt. The obtained result from FT-IR spectra and SEM micrographs indicates that the PSt and PMMA chains have been covalently attached onto the MWCNTs. TEM indicates that the initiation and dissemination of polymerization were created not only at the apex’s, as well as on the outer walls of the CNTs. Furthermore, the coaxial nanostructure of the final MWCNT-g-PMMA-b-PSt is considered. The thermal stability of PMMA by nanotubes was improved. Also, the results imply that the thermal degradation of PSt is delayed by the connection of MWCNTs into PSt as covalent bonding owing to the restriction effect of MWCNTs on the PSt chains and the high thermal stability of MWCNTs in MWCNT-g-PMMA-b-PSt.

5. Acknowledgment

The author expresses their gratitude to the Tabriz Payame Noor University for supporting of this project.

References

[1] W. Chen, L. Huang, J. Hu, T. Li, F. Jia, Y.F. Song, Phys. Chem. Chem. Phys.,16, 19668 (2014)

[2] M. R. Jalali Sarvestani, R. Ahmadi, B. Farhang Rik, Chem Rev Lett., 3,175 (2020)

[3] M. M. Samya, M.G. Mohamed, S.W. Kuoac, Compos Sci Technol., 199, 108360 (2020)

[4] M. He, S. Zhang, J. Zhang, Chem. Rev., 120, 12592 (2020)

[5] Yu. Sun, Y. Yang, X.L. Shi, G. Suo, H. Chen, X. Hou, S. Lu, Z.G. Chen, ACS Appl. Mater. Interfaces, 13, 28359 (2021)

[6] J. Hua, C.X. Hong, T.X. Dong, C. M. Wang, Composites Part A., 140, 106188 (2021)

[7] M. V. Il'ina, O. I. Il'ina, Y. F. Blinov, A. A. Konshin, B. G. Konoplev, O.A. Ageev, Materials., 11, 638 (2018)

[8] K.Sun, P.Xie, Z.Wang, T. Su, Q.Shao, J.E. Ryue, X. Zhang, J.Guo, A. Shankare, J. L, R. fan, D. Cao, Z. Guo, Polymer., 125,50 (2017)

[9] M.A. Tasdelen, M.U. Kahveci, Y. Yagci, Prog. Polym. Sci., 36, 455 (2011)

[10] S. Ghasemi Karaj-Abad, M. Abbasian, M. Jaymand, Carbohydr polym, 152, 297 (2016)

[11] H. Rafiei, M. Abbasian, R. Yegani, Iran. Polym. J., 29, 371 (2020)

[12] M. Abbasian, M. Bakhshi, M. Jaymand, S. Ghasemi Karaj-Abad, J. Elastom. Plast, 51, 473 (2019)

[13] M. Abbasian, M. Seyyedi, M. Jaymand, Polym Bull., 77, 1107 (2020)

[14] M.H. Valiollahi, M. Abbasian, M. Pakzad, Iranian journal of chemistry and chemical engineering (IJCCE), 38, 55 (2019)

[15] R. Mohammad-Rezaei, B. Massoumi, M. Abbasian, M. Eskandani, M. Jaymand, J. Mater. Sci., 30, 2821 (2019)

[16] B. Massoumi, Abbasian M, R. Mohammad-Rezaei, A. Farnudiyan-Habibi, M. Jaymand, Polym. Adv. Technol., 30, 1484 (2019)

[17 M. Maghsoudi, M. Abbasian, K. Farhadi, J. Elastom. Plast., 53,469 (2021).

[18] M. Abbasian, P. Hasanzadeh, F. Mahmoodzadeh, R. Salehi, J. Macromol. Sci. Part A., 57, 99 (2020)

[19] M. Abbasian, L. Razavi, M. Jaymand, S. Ghasemi Karaj-Abad, Scientia Iranica., 26, 1447 (2019)

[20] M. Hosseinzadeh, M. Abbasian, L. Ghodsi, S. Ghasemi Karaj-Abad, M. Hayri Acar, F. Mahmoodzadeh, M. Jaymand, ChemistrySelect, 7, e202104228 (2022)

[21] M. Abbasian, R. Mahi, J. Exp. Nanosci., 9, 785 (2014)

[22] M. Abbasian, M. Jaymand, M.Z. Ghadami, A. Fathi, Int. J. Nanosci. Nanotechnol, 6, 168 (2010)

[23] M. Abbasian, J. Elast. Plast, 43, 481 (2011)

[24] L. Ouyang, L. Wang, F.J. Schork, Polymer, 52, 63 (2011)

[25] Summerlin, B.S.; Tsarevsky, N.V.; Louche, G.; Matyjaszewski, K.; Lee, R.Y. Macromolecules, 38, 7540 (2005)

[26] M. llcíkova, M. Mrlík, T. Sedlcek, M. Doroshenko, K. Koynov, M. Danko, J. Mosncek, Polymer, 72, 368 (2015)

[27] A.E. Daugaard, K. Jankova, S. Hvilsted, polymer, 55,481(2015)

[28] D.Q. Fan, J.P. He, W. Tang, J.T. Xu, Y.L. Yang, Eur. Polym. J., 43, 26 (2007)

[29] M. Jaymand, Polymer, 52, 4760 (2011)

[30] M. Hatamzadeh, M. Jaymand, B. Massoumi, Polym. International, 63, 402 (2014)

[31] S. Ghasemi Karaj-Abad, M. Abbasian, M. Hosseinzadeh, S. Nasry Saheb, S. Esmaeily Shoja Bonab, J. Nanostruct., 11, (2022) Available online in https://jns.kashanu.ac.ir/article_111920.html

[32] C.J Hawker, G.G. Barcley, A. Orellana, J. Dao, W. Devonport, Macromolecules., 29, 5245 (1996)

[33] M. Abbasian, M. Shahparian, S. Esmaeily Shoja Bonab, Iran. Polym. J., 22, 209 (2013).

How to Cite This Article
Mojtaba Abbasian, Saber Ghasemi Karaj-Abad, Mehdi Hosseinzadeh, Shiva Asadi and Solmaz Esmaeily Shoja, “Synthesis and characterization of poly methyl methacrylate-b-polystyrene copolymer/ multi -walled carbon nanotubes via ATRP and NMRP techniques” International Journal of New Chemistry., 10 (2), 65-83. 2023; DOI: 10.22034/ijnc.2022.551988.1266

2